Iranian Journal of Chemical Engineering

Journal Homepage: www.ijche.com

pISSN: 1735-5397
eISSN: 2008-2355

Regular Article

Optimization of the Homogeneous Rhodium-Catalyzed Methanol Carbonylation Reactor to Reduce CO_2 Emissions

A. H. Oudi, R. Golhosseini *

Department of Chemical Engineering, Faculty of Engineering, University of Kashan, P. O. Box: 873175-1167, Kashan, Iran

ARTICLE INFO

Article history:
Received: 2022-10-04
Accepted: 2023-01-28
Available online: 2023-01-29

Keywords:
Carbon Emission Reduction,
Optimization,
Rhodium-Catalyzed,
Homogeneous Methanol Carbonylation,
Central Composite Design

ABSTRACT

The optimization of the homogeneous rhodium-catalyzed methanol carbonylation reactor to reduce CO_2 emissions was studied in this line of research. The average relative error of 4.8 percent between the simulation and industrial results indicates the accuracy of the simulation. The central composite design (CCD) and genetic algorithm (GA) with the aid of a simplified simulation process using Aspen HysysV.9 software were used to evaluate the effect of individual variables (the liquid level, the temperature of the catalyst-rich recycle stream, the mole ratio of CO to methanol (MeOH) in the feed, and the flow rate of the dilute acid stream) and their mutual interactions to reduce CO_2 emissions. It was obtained that the liquid level of 46 %, the catalyst-rich recycle stream temperature of 120 °C, the CO: MeOH molar ratio equal to 1.13:1, and the dilute acid flow rate of 513.14 kmol/h lead to the CO_2 reduction by 34 %.

DOI: 10.22034/ijche.2023.364482.1459 URL: https://www.ijche.com/article_165983.html

1. Introduction

In the industrial setting, chemical interactions between the gas and liquid phases are common. These reactions take place in a tank or column reactor. Numerous variables, such as the reaction kinetics, mass transfer, and heat transfer influence the reactor type [1-4]. Bao et al. [5] conducted an experimental study on the effect of the diameter of stirrers on the gas dispersion rate and bubble size inside the gas-liquid reactor. They concluded that if the surface velocity of the gas is low, the diameter of the stirrer impeller does not have much effect on the gas retention, but if the surface velocity of the gas is high, the diameter of the agitator impellers has a significant effect on the gas retention. In other words, the smaller the diameter of the stirrer impeller, the faster the stirrer, resulting in smaller bubbles and an increase in the gas retention. In recent years, mass transfer coefficient predictions in gas-liquid stirred reactors have been investigated

*Corresponding author: rgolhosseini@kashanu.ac.ir (R. Golhosseini)

in various processes [6-12].

AcOH is a key petrochemical intermediate that is used to make vinyl acetate, acetic anhydride monomers, and the terephthalic acid solvent [13]; and synthesized in a stirred gas-liquid reactor. According to the data, the amount of the AcOH production increases from 18 million tons to 20.3 million tons in 2020-2024 [14]. Methanol carbonylation in the vapor phase [15], methyl formate isomerization [16], the direct carbonylation of methane [17], the homogeneous carbonylation of methanol in the liquid phase, as the most common mass production method, and the fermentation are all methods of producing AcOH [18]. The homogeneous carbonylation of methanol performed at a temperature of 180-220 °C and a pressure of 30-40 atm having used a methyl iodide promoter and a rhodium catalyst was commercialized by the Monsanto in 1973. Also in this method, the yield of AcOH is up to 99 % based on the consumption of methanol and 85 % for CO and the selectivity of AcOH based on methanol is 100 % [19]. Electrolyte additives such as lithium iodide and sodium iodide added by the Celanese resulted in a reduction of water content in the preferred process system (H_2O < 2-3 wt %). [20, 21]. In 1996, BP developed the Cativa process, which uses an iridium catalyst at a process with low content of water [22]. The Monsanto process uses a lot of water (14-15 wt %) to prevent the precipitation of the catalyst, which increases the cost of separating the water in downstream. In a study by Zhang et al. [23] the ionic liquid-supported homogeneous carbonylation of methanol over Ir (III) catalysts was used to produce AcOH in the non-aqueous liquid phase. It was found that 1-butyl-3-methylimidazolium bis (trifluoromethanesulfonyl)imide ([Bmim]Tf2N) and N-butylpyridinium bis (trifluoromethanesulfonyl)imide ([BPy]Tf2N) could promote the AcOH selectivity (> 98 %) and methanol conversion (> 99 %) under the relatively mild reaction condition of 160 °C and 3.0 MPa. In the study of Ji et al. [24], the findings of the experiments showed that the Rh(I)-o-aminophenol catalyst produced more AcOH and lost less rhodium during the catalysis process. As a result, the Rh(I)-o-aminophenol catalyst is a more active and stable catalytic system and the optimal amount of water is 6 wt %.

Damian and Case [25] investigated the Monsanto process from the perspective of the process energy integration, which demonstrated a reduction in greenhouse gas emissions in that case. Caxiano et al. [26] simulated the purification section of Monsanto process and examined the different column sequence of separation towers, selected the best sequence that was more economical, energy-efficient, and environmentally friendly than the original sequence.

CO_2 formed by the water-gas shifting reaction (WGSR) is one of the undesirable byproducts in the carbonylation reactor. One of the most pressing environmental concerns in the world today is the excessive rise in the effects of greenhouse gases such as CO_2, which have increased by 25 % since the beginning of industrialization around 200 years ago [27]. Greenhouse gases are the major contributor to the global warming. According to the US Environmental Protection Agency, CO_2 accounts for about 82 % of greenhouse gases [28, 29]. Medrano-Garcia et al. [30] explored seven different methods of producing AcOH to reduce CO_2 emissions and reduce the economic costs of the process. They also suggested that some of the H_2 produced be recycled to the reactor to reduce the rate of the WGSR and thus lower the production rate of

CO_2.

Considering the great importance of environmental issues and the importance of reducing CO_2 emissions, the effects of various operating parameters and reactor optimization on the homogeneous rhodium-catalyzed methanol carbonylation are studied quantitatively and qualitatively.

First, the reactor was simulated in AspenHysys.V9 software. In the following, a statistical relationship between independent variables and the amount of CO_2 emission which was obtained with the aid of the design of experiments (DOE) method received a lot of attention in recent decade [31-33]. Then, the optimal values of independent variables to minimize CO_2 emissions were obtained by GA which is a common method for optimization [34-42].

2. Methodology

2.1. Chemistry of the process and overview of engineering the reaction

The homogeneous rhodium-catalyzed methanol carbonylation is a very slow reaction, and the gas-liquid mass transfer effects are negligible [43]. Hatta number (Ha) is a dimensionless parameter that compares the reaction rate in a liquid film to the rate of diffusion through the film. It can be considered also as the ratio of the gas-liquid contact-time to the reaction time [44-46]. The value of the Ha at the CSTR of the Monsanto process is very small. If Ha is very small, no reaction occurs in the film, and the bulk volume becomes the rate controlling factor, all we need is a large volume of liquid, whereas agitation to create large interfacial areas is of no benefit here and the rate is determined by chemical kinetics alone [47]. The evidence of the above mentioned reasons is the low agitation speed (~ 80 rpm) and large volume of the liquid reaction phase (~ 50 m^3) of the reactor at the Monsanto process. Therefore, the investigation and modeling of the gas-liquid mass transfer do not matter. Due to instability issues, the reaction rate of the homogeneous rhodium-catalyzed methanol carbonylation is less than its theoretical value. This value is approximately equal to 60 % of the theoretical value. The lack of the familiarity with and the consideration of this subject in simulation leads to inappropriate conclusions [48]. The schematic cycle of the interrelated organometallic reaction path for the rhodium-catalyzed methanol carbonylation to AcOH (chemical equation 1) [49] is shown in Figure 1.

$$CH_3OH + CO \rightarrow CH_3COOH \quad (1)$$

(a)

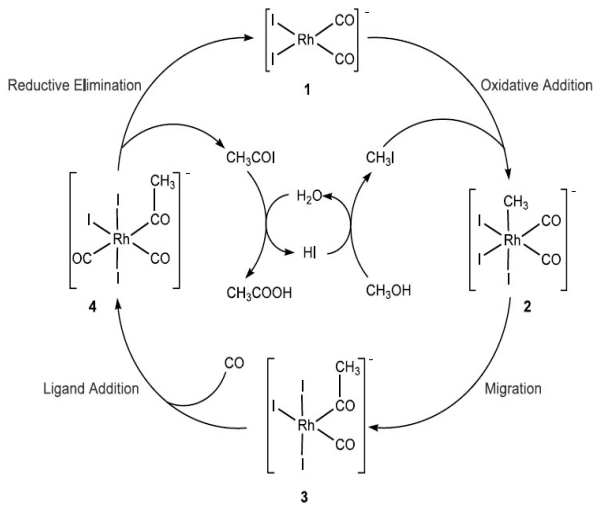

(b)

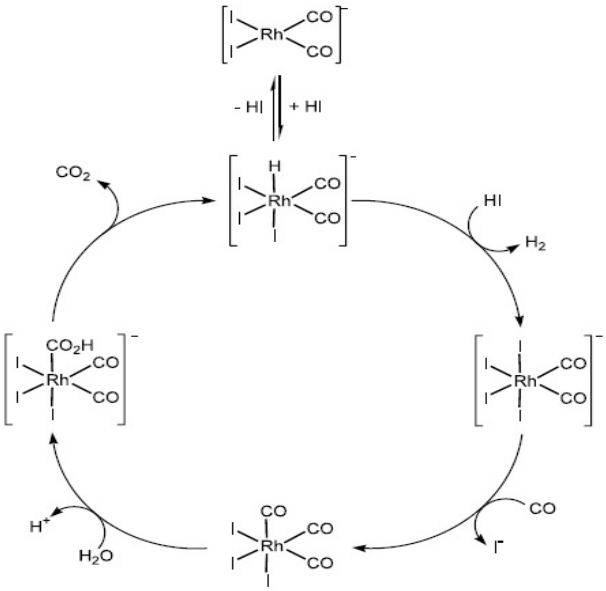

Figure 1. Catalytic cycle of the rhodium-catalyzed (a) methanol carbonylation and (b) water-gas shift reaction [50].

While water is essential for steps 2 and 6, the higher content of water would mean the loss of CO by WGSR (chemical equation 7) [51].

$$CH_3OH + HI \rightleftharpoons CH_3I + H_2O \quad (2)$$

$$CH_3I + RhI_2(CO)_2^- \longrightarrow CH_3RhI_3(CO)_2^- \quad (3)$$

$$CO + CH_3RhI_3(CO)_2^- \longrightarrow CH_3C(O)RhI_3(CO)_2^- \quad (4)$$

$$CH_3C(O)RhI_3(CO)_2^- \longrightarrow RhI_2(CO)_2^- + CH_3COI \quad (5)$$

$$CH_3COI + H_2O \rightleftharpoons CH_3COOH + HI \quad (6)$$

$$CO + H_2O \rightleftarrows H_2 + CO_2 \quad (7)$$

HI also can form byproducts as shown in equations 8-9:

$$CH_3RhI_3(CO)_2^- + HI \longrightarrow CH_4 + RhI_4(CO)_2^- \quad (8)$$

$$RhI_2(CO)_2^- + 2HI \rightleftharpoons H_2 + RhI_4(CO)_2^- \quad (9)$$

In equations 8-9, Rh(I) is getting oxidized to Rh(III) which is to be reduced back to Rh(I) by water & CO as in equation 7 Rh(III) where Iodide may precipitate in the absence of water. According to chemical equation 10, methanol is first converted to methyl acetate and water through esterification with AcOH and then carbonylated by equation 11.

$$CH_3COOH + CH_3OH \rightarrow CH_3COOCH_3 + H_2O \quad (10)$$

$$CH_3COOCH_3 + CO + H_2O \rightarrow 2CH_3COOH \quad (11)$$

Equation 12 expresses the dependence of the rate of homogeneous carbonylation of methanol reaction on the components. The coefficients m and n are stated differently

depending on whether the reaction environment is acidic or aqueous (See Table 1) [52]:

$$\text{Rate} \propto [\text{Rh}][\text{I}][\text{CO}]^{\text{m}}[\text{CH}_3\text{OH}]^{\text{n}} \quad (12)$$

where [Rh] is the concentration of the rhodium catalyst and [I] is the concentration of methyl Iodide (kmol/m^3) in the reaction.

Table 1
Values of coefficients a and b in the carbonylation reaction rate.

Coefficients	Aquatic environment		Acidic environment	
	$P_{CO} > 10$	$P_{CO} < 10$	$P_{CO} > 10$	$P_{CO} < 10$
m	0	1	0	1
n	0.64	0.64	0	0

Since the reaction medium is acidic and the partial pressure of CO is greater than 10 bar, according to Table 1, the kinetics for the homogeneous carbonylation of the methanol reaction is expressed according to equation 13 [53]:

$$\text{Rate} = 158800000 \times \exp\left(\frac{-72200}{\text{RT}}\right) \times [\text{I}] \times [\text{Rh}] \quad (13)$$

Equation 14 also shows the rate of WGSR [54]:

$$\text{Rate} = 146664 \times \exp\left(\frac{-71407}{\text{RT}}\right) \times [\text{I}]^{1.055} \times [\text{Rh}]^{1.0096} \quad (14)$$

Equation 15 is used to determine the equilibrium constant of WGSR [55].

$$\ln\text{K} = -12.11 + \frac{5319}{\text{T}} + 1.012 \ln\text{T} + 1.144 \times 10^{-4}\,\text{T} \quad (15)$$

2.2. Battery limits

The inlet flow streams to the reactor (CO (21004-21020), Methanol-Mix, catalyst-rich recycle stream (21010), recycle flow of the liquid separated (21007), dilute acid from the purification section and heavy phase flow are depicted in Figure 2.

The liquid product (L) and the output stream from the reactor's gas phase of which part is wasted and the rest enters the flash drum and is divided into two streams (21007), are the output flow streams from the reactor.

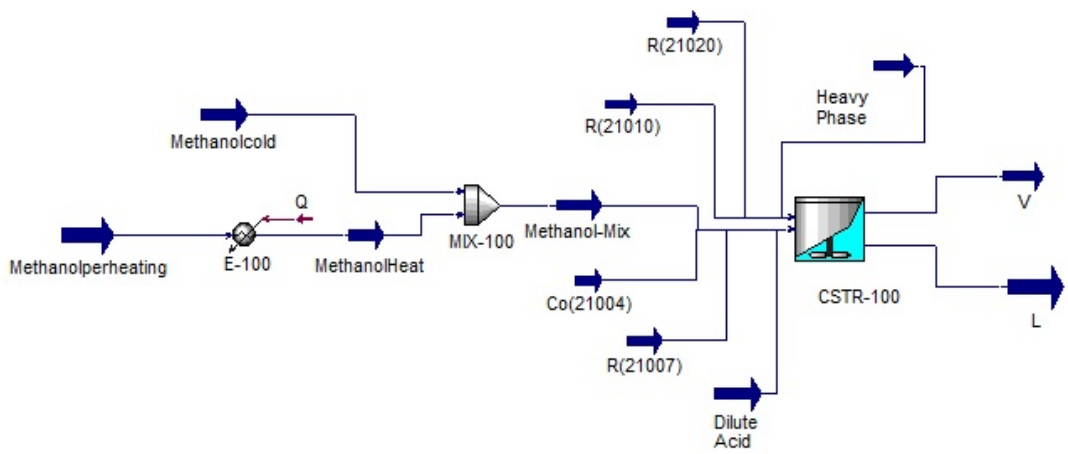

Figure 2. Scheme of the reaction part of the Monsanto process.

2.3. Design of experiments

DOE includes a series of experiments that designedly make changes in process input variables to reveal their effect on the output variable. In this research, the central composite design (CCD) method has been used in five levels. The advantage of this method over other methods is that it is an economical method and does not require much data for modeling. To express a mathematical relationship between dependent and independent variables, first data must be collected using experiments or precise simulations, and then regression analysis is used to examine the relationship between the response variable and the factors affecting the response. To analyze regression and determine the regression model and estimate the model parameters, the least squares method, according to equation 16, can be used [56]:

$$y = \beta_0 + \sum_{i=1}^{k} \beta_i x_i + \sum_{i=1}^{k} \beta_{ii} x_i^2 + \sum_{1 \le i \le j}^{k} \beta_{ij} x_i x_j + \varepsilon \qquad (16)$$

In equation 16, β is the matrix of coefficients, ε is the error value, x is the independent variable, y is the dependent variable, and i, j and k are the numerators of the independent variables.

3. Results and discussion

3.1. Steady-state simulation

According to Figure 2, the process is simulated using Aspen Hysys V.9 software. The NRTL equation of state (EOS) is used to evaluate the properties of the liquid phase due to the non-ideality of the reaction medium, and the Virial EOS is used to evaluate the physical properties of the vapor phase [57].

The simulation results of the reactor (59.26 m^3 volume) and operational data are compared and validated in Table 2.

Table 2
Comparison of simulation results with operational data.

Component	Design	Simulation	Deviation (%)
T (°C)	185.00	191.20	3.35
P (bar)	28.60	28.60	0
H_2	0.03	0.02	33.30
CO	0.22	0.22	0
CO_2	0.08	0.08	0
CH_3OH	0.056	0	-
CH_3I	3.52	3.56	1.10
CH_3COOCH_3	0.60	0.64	6.30
CH_3COOH	55.86	56.09	0.41
H_2O	38.31	38.16	0.39
HI	1.19	1.15	3.36

3.2. Effective operational parameters

3.2.1. Temperature of the catalyst-rich recycle stream

The rate of WGSR decreases as the temperature of the catalyst-rich recycle stream to the reactor decreases, but it is important to note that reducing the reactor temperature to less than 180 °C increases the amount of

methyl acetate, resulting in the precipitation of the catalyst. As shown in Figure 3, the lower limit of the temperature of the recycle flow is 120 °C, while the upper limit is 127.5 °C [58].

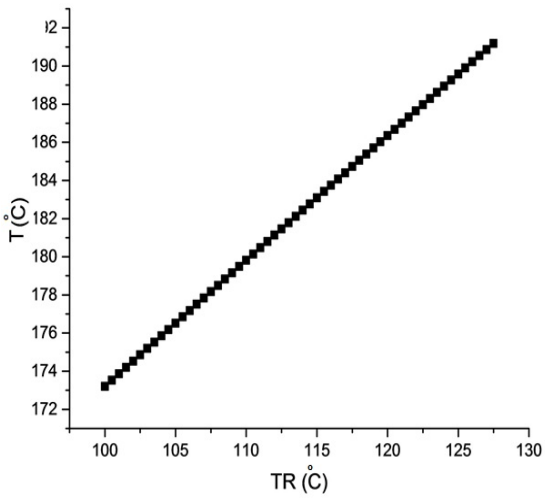

Figure 3. Effect Temperature of the catalyst-rich recycle stream on the reactor temperature.

3.2.2. Liquid level

The normal level of the liquid in the reactor is 3450 mm and outside the range of 1727-3506 mm which causes an alarm in the reactor level control system, therefore, the liquid level inside the reactor should be in the range of 30-62 % [58]. The reactor level is regulated by recycle flows. The liquid holdup has a direct effect on the gas holdup in the reaction phase. If the liquid holdup in the reactor decreases, the production rate of acetic acid does not change much, but the production rate of CO_2 decreases as shown in Figure 4.

3.2.3. Flow rate of the dilute acid stream

Considering that the weight percentage of water in the reactor should always be 14-15 w % (Figure 5) and also the amount of the AcOH production should not be reduced (Figure 6), its lower and upper bounds are selected as 513 $\frac{\text{kmol}}{\text{h}}$ and 561.3 $\frac{\text{kmol}}{\text{h}}$ respectively. It should be noted that the liquid level inside the reactor is controlled by the flow rate of the diluted acid from the purification section [58].

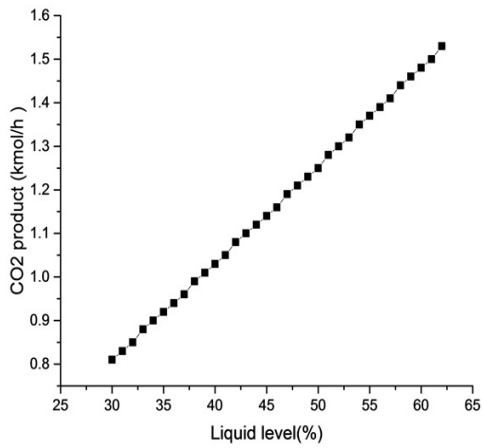

Figure 4. Effect of the liquid level on the production of CO_2.

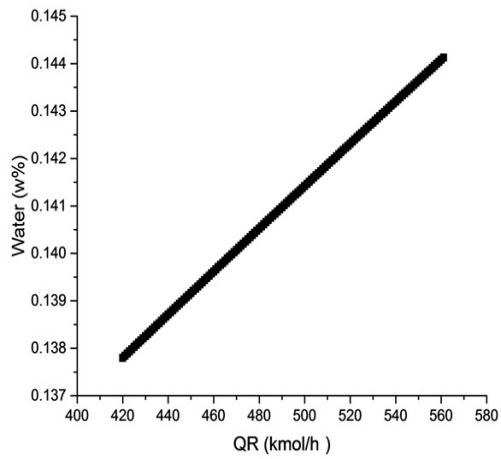

Figure 5. Effect of the flow rate of the dilute acid stream on the amount of water in the reactor.

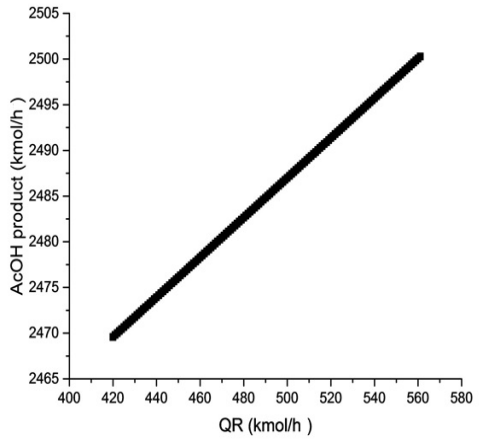

Figure 6. Effect of the flow rate of the dilute acid stream on the AcOH production.

3.2.4. Feed ratio of CO to methanol

Conforming to the minimum partial pressure of 10 bar of CO and its selectivity, and the reactor temperature limit which should not be less than 180 °C, the minimum and maximum ratio of CO to the methanol feed can be 1.13 and 1.21 respectively [58].

3.3. Design of Experiments

One of the common methods for designing experiments is the central composite method (CCD). This method is performed in 5 levels +α, +1, 0,-1 and -α, which are designed for +1 and -1 points on the surfaces, 0 central points and +α and -α axial points respectively [59]. In this work, the Design-Expert V.10 software has been used to design experiments. Table 3 shows the levels selected for the independent variables in the CCD method. Table 4 also shows the experiments performed and the resulted amounts of CO_2 and AcOH produced for each test.

Table 3

Levels and experimental ranges for the independent variables or factors.

Factor	Range and levels				
	−α	**-1**	**0**	**1**	**+α**
Temperature of the catalyst-rich recycle stream	385.5	388	390.5	393	395.5
Liquid level	0.2	0.4	0.6	0.8	1
Flow rate of dilute acid stream	225	300	375	450	525
Feed ratio of CO to methanol	1.6	1.8	2	2.2	2.4

Table 4

Natural values and outcomes of the experimental design matrix.

Run	T_R (K)	L_C	Q_R ($\frac{kmol}{h}$)	F_{12}	CO_2 ($\frac{kmol}{h}$)	AcOH ($\frac{kmol}{h}$)
1	390.5	0.6	225	2.0	0.9688	**180.8**
2	393.0	0.8	450	2.2	0.9488	**164.9**
3	393.0	0.8	450	1.8	1.4220	**201.1**
4	393.0	0.4	300	2.2	0.5325	**164.6**
5	393.0	0.4	300	1.8	0.8235	**200.8**
6	385.5	0.6	375	2.0	0.7306	**181.0**
7	390.5	0.6	375	2.0	0.8364	**181.0**
8	393.0	0.8	300	1.8	1.6470	**200.8**
9	390.5	0.6	375	2.0	0.8364	**181.0**
10	388.0	0.8	450	2.2	0.8092	**164.9**
11	390.5	1	375	2.0	1.3940	**181.0**
12	390.5	0.6	375	2.0	0.8364	**181.0**
13	393.0	0.8	300	2.2	1.0650	**164.6**
14	390.5	0.6	375	2.4	0.5967	**151.2**
15	388.0	0.4	300	1.8	0.7051	**200.8**
16	390.5	0.6	375	1.6	1.4210	**225.8**
17	390.5	0.2	375	2.0	0.2788	**181.0**
18	388.0	0.8	300	1.8	1.4100	**200.8**
19	388.0	0.4	450	2.2	0.4046	**164.9**
20	390.5	0.6	375	2.0	0.8364	**181.0**

21	390.5	0.6	375	2.0	0.8364	**181.0**
22	388.0	0.4	450	1.8	0.6093	**201.1**
23	390.5	0.6	375	2.0	0.8364	**181.0**
24	393.0	0.4	450	1.8	0.7112	**201.1**
25	390.5	0.6	525	2.0	0.7366	**181.3**
26	388.0	0.8	300	2.2	0.9311	**164.6**
27	388.0	0.8	450	1.8	1.2180	**201.1**
28	388.0	0.4	300	2.2	0.4651	**164.6**
29	393.0	0.4	450	2.2	0.4744	**164.9**
30	395.5	0.6	375	2.0	0.9802	**181.0**

3.4. Analysis of variance

Equations 17 and 18 show the production of CO_2 ($\frac{\mathbf{kmol}}{\mathbf{h}}$) and AcOH ($\frac{\mathbf{kmol}}{\mathbf{h}}$) respectively:

$$\begin{aligned} CO_2 = {} & 85.57806 - 0.47868T_R - 12.41987L_C + 2.67729\times10^{-3}Q_R + 7.49883F_{12} \\ & + 0.044625T_RL_C - 1.38\times10^{-5}T_RQ_R - 0.031325T_RF_{12} - 1.36833\times10^{-3}L_CQ_R \\ & - 1.51625L_CF_{12} + 1.11833\times10^{-3}Q_RF_{12} + 6.99\times10^{-4}T_R^2 - 9.53125\times10^{-3}L_C^2 \\ & + 6.56667\times10^{-7}Q_R^2 + 1.06828F_{12}^2 \end{aligned} \tag{17}$$

$$\begin{aligned} AcOH = {} & 397.60975 + 0.781T_R + 0.18750L_C + 1.05556\times10^{-3}Q_R - 278.29167F_{12} \\ & + 1.53205\times10^{-13}T_RL_C + 3.59279\times10^{-16}T_RQ_R + 7.10055\times10^{-14}T_RF_{12} \\ & + 5.49599\times10^{-15}L_CQ_R + 2.10166\times10^{-12}L_CF_{12} + 6.01364\times10^{-15}Q_RF_{12} \\ & - 1\times10^{-3}T_R^2 - 0.15625L_C^2 + 1.11111\times10^{-6}Q_R^2 + 46.71875F_{12}^2 \end{aligned} \tag{18}$$

In equations 17 and 18, T_R is the temperature of the catalyst-rich recycle stream (K), L_C is the liquid level, Q_R is the flow rate of the dilute acid stream ($\frac{\mathrm{kmol}}{\mathrm{h}}$) and F_{12} is the feed ratio of CO to methanol.

Figure 7 shows the correlation between the actual values and the predicted values, which indicates a good match between the predicted values and the actual values.

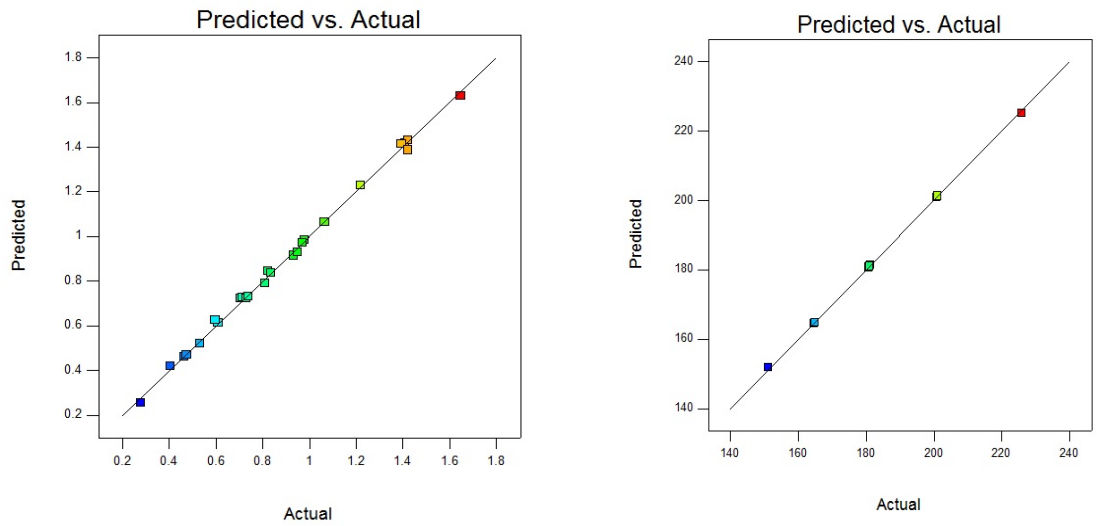

(a) (b)

Figure 7. Plot of the predicted response vs. a) the CO_2 production b) the AcOH production.

According to equation 19, the F-Value used for the analysis of the variance is defined as the ratio of the mean squares of the effect (MS_{effect}) to the mean squares of the error (MS_{error}).

$$F = \frac{MS_{effect}}{MS_{error}} \quad (19)$$

Tables 5 and 6 show the F-Values and P-Values for the obtained model. With effective factors, the p values for Fisher's exact test are less than the significant level of 0.05 [60, 61].

Table 5
Effectiveness of the selected variables on the amount of the CO_2 production.

Variable	F-Value	P-Value
Model	584.20	< 0.0001
T_R	262.30	< 0.0001
L_C	5140.78	< 0.0001
Q_R	222.22	< 0.0001
F_{12}	2213.23	< 0.0001
$T_R L_C$	20.31	0.0004
$T_R Q_R$	0.27	0.6088
$T_R F_{12}$	10.01	0.0064
$L_C Q_R$	17.19	0.0009
$L_C F_{12}$	150.08	< 0.0001
$Q_R F_{12}$	11.48	0.0041
T_R^2	1.33	0.2660
L_C^2	0.01	0.9210
Q_R^2	0.95	0.3441
F_{12}^2	127.71	< 0.0001

3.5. Analysis of the dependence of the CO_2 production on independent variables

Figure 8 shows that increasing the flow rate of the dilute acid and decreasing the liquid level in the reactor reduce the production of CO_2, but because the liquid level in the reactor is controlled by the flow rate of the dilute acid [62], so if we want to decreased the liquid level in the reactor we must reduce the amount of the flow rate of the dilute acid (assuming the other parameters remain the same). As shown in the studies of Baker et al [63], it is also clear from Figure 9 that as the temperature of the catalyst-rich recycle stream decreases, the reactor temperature decreases and the amount of the CO_2 production decreases, as does the feed ratio of CO to methanol, because the larger the ratio, the decreased the methanol feed flow rate. And because the reactor temperature is controlled by the flow rate of the methanol feed, by reducing the methanol feed flow rate the reactor temperature decreases, so does the amount of the CO_2 production. However, it should be noted that changing the flow rate of the methanol feed stream requires controlling the stability of the reactor temperature, and the AcOH reactor is very sensitive to temperature changes.

Table 6
Effectiveness of selected variables on the production of AcOH.

Variable	F-Value	P-Value
Model	5359.14	< 0.0001
T_R	0	1
L_C	0	1
Q_R	4.45	0.0522
F_{12}	74093.94	< 0.0001
$T_R L_C$	0	1
$T_R Q_R$	0	1
$T_R F_{12}$	0	1
$L_C Q_R$	0	1
$L_C F_{12}$	0	1
$Q_R F_{12}$	0	1
T_R^2	9.895×10^{-3}	0.9221
L_C^2	9.895×10^{-3}	0.9221
Q_R^2	9.895×10^{-3}	0.9221
F_{12}^2	884.64	< 0.0001

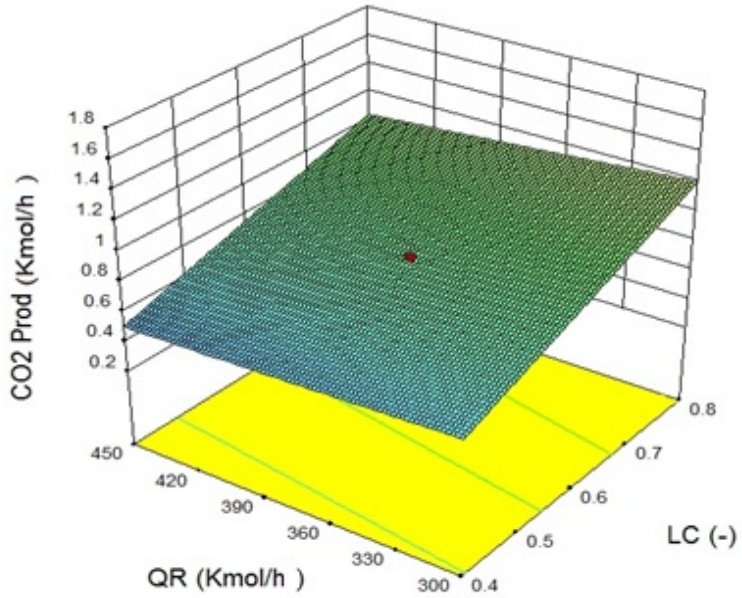

Figure 8. Changes in CO_2 emissions due to the flow rate of the dilute acid and the level of the liquid in the reactor.

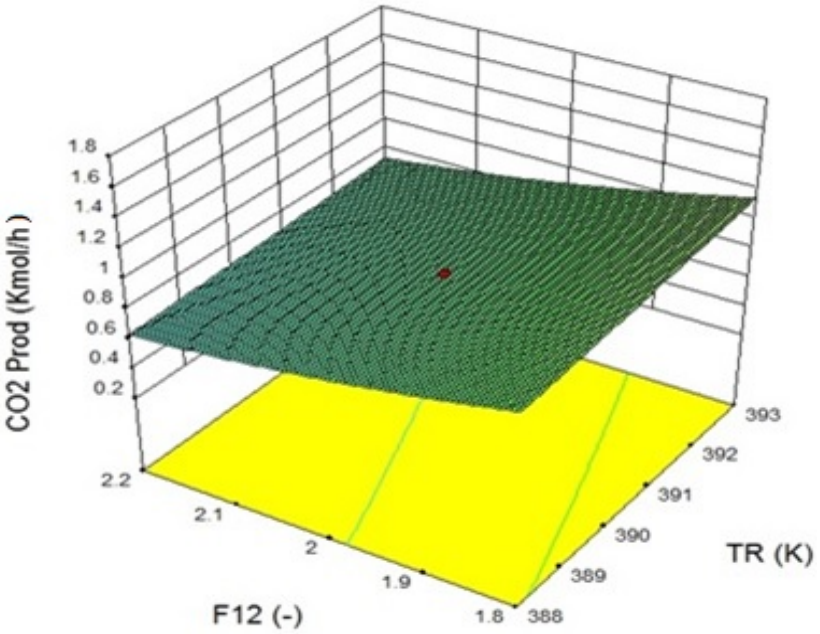

Figure 9. Changes in the CO_2 production due to the temperature of the catalyst-rich recycle stream and the feed ratio of CO to methanol.

Figure 10 shows the contour plots of the second order model for each response. Non-linear appearance of contour curves implies strong interaction. As it can be seen in these figures, the interaction between two parameters of the feed ratio of CO to methanol and the liquid level is significant. The amount of each response is obvious in each plot; moreover, the appropriate range of parameters is obvious in contour plots.

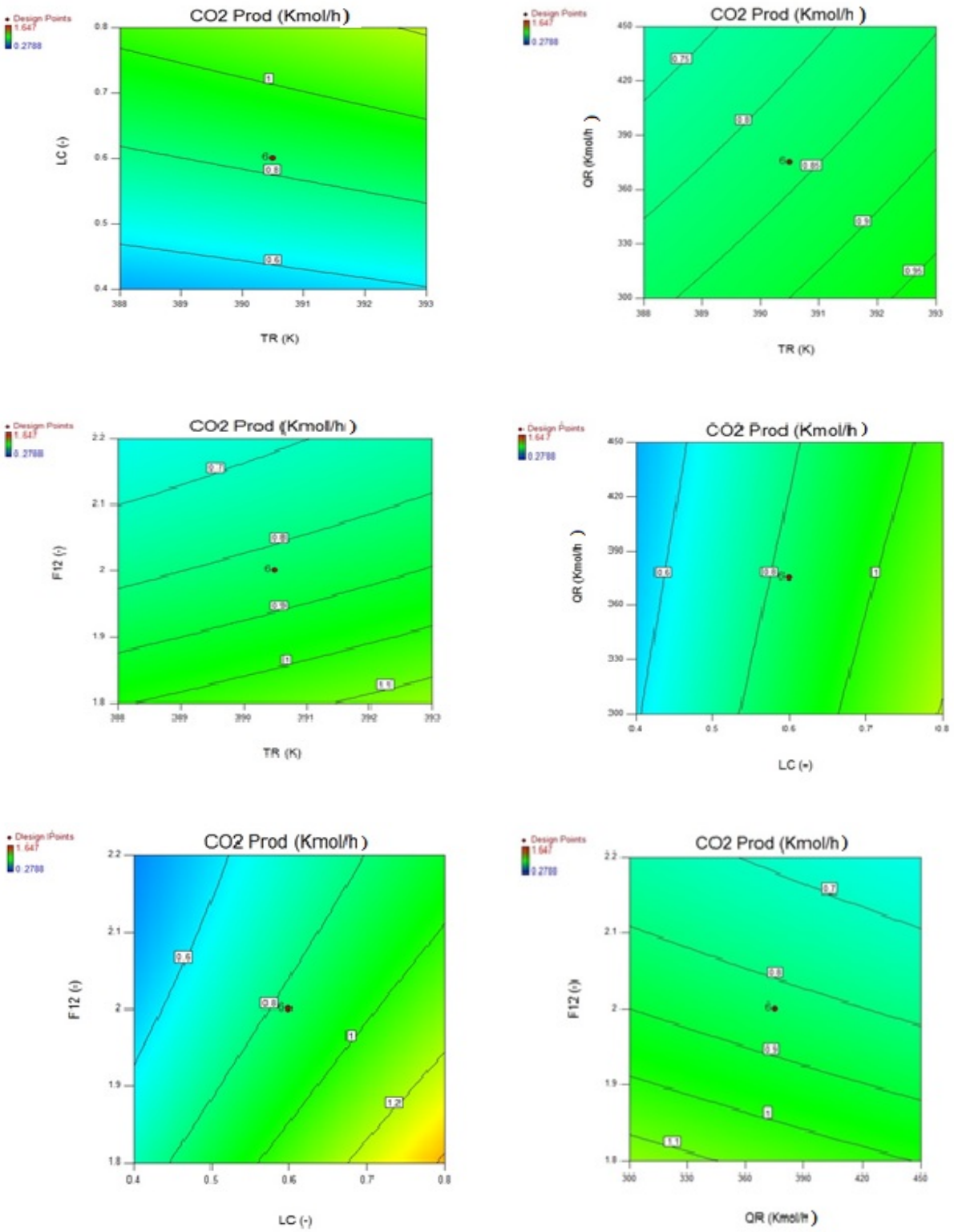

Figure 10. Contour plots of the second order model for the CO_2 production.

3.6. Optimization

In the multi-objective optimization, because a response cannot always lead to an optimal solution for all objective functions, the concept of Pareto Front is used for optimization. Pareto Front is a front of justified answers that includes the best possible answer to the optimization problem among all possible

answers, and finally in the multi-objective optimization by the best answer overcoming other answers from the Pareto Front. To achieve the objectives of the problem, optimization is done. To obtain the best available answer from Pareto Front, we used the gamultiobj toolbox in the MATLAB software for the multi-objective optimization using a genetic algorithm [64]. Table 7 shows the optimal values of the operating parameters for minimizing the amount of the CO_2 production (objective function of Equation (17)) and maximizing the amount of the AcOH production (objective function of Equation (18)). It is determined that a 46 % level of the liquid , the catalyst-rich recycle stream temperature of 120 °C, a CO: MeOH molar ratio of 1.13:1, and a flow rate of 513.14 kmol/h of the dilute acid stream result in a 34 % reduction in the CO_2 production. In the work of Hosseinpour et al [65] DOE in conjunction with the response surface methodology (RSM) was used to investigate the effects of seven factors, including temperature, pressure, and the concentrations of iridium, ruthenium, methyl iodide, methyl acetate, and water, on the formation of H_2 and CO_2 as the result of the water-gas shifting reaction and other side reactions in the Ir-catalyzed methanol carbonylation process. Experiments were designed using a central composite design at five levels. It was shown that increasing the pressure and amount of methyl iodide decreased the formation of CO_2, while an increase in the amount of other factors promoted the formation of CO_2.

As shown in Figure 11, the CO_2 production decreases from 4.340 $\frac{\text{kmol}}{\text{h}}$ to 2.847 $\frac{\text{kmol}}{\text{h}}$.

Table 7
Optimal operating parameters of the AcOH reactor.

Parameters	Lower bound	Upper bound	Current value	Optimal value
T_R (°C)	120	127.5	127.5	120
L_C ($\times 10^2$)	30	62	61	46
Q_R ($\frac{\text{kmol}}{\text{h}}$)	513	561.3	561.3	513.14
F_{12}	1.13	1.21	1.13	1.13

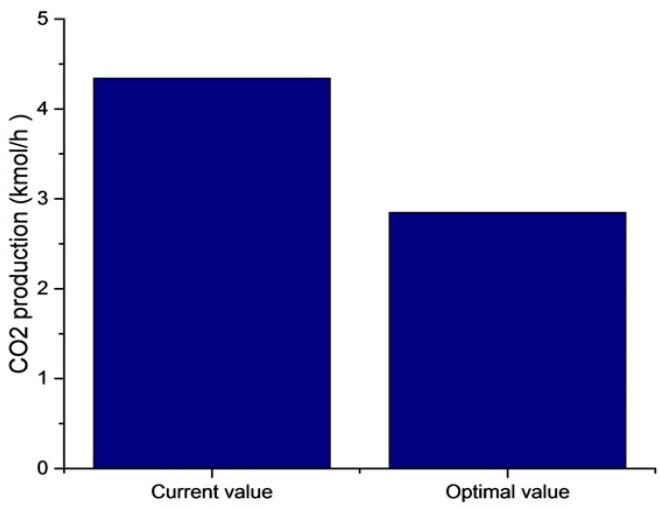

Figure 11. Current value vs. optimal value for the CO_2 production.

4. Conclusions

The simulation of the homogeneous carbonylation reactor and DOE by CCD using the Design Expert software (v.10) led to the detailed analysis and investigation of the effect of selected parameters on the CO_2 production rate. The results showed that reducing the liquid level in the reactor from 61 % to 46 %, the catalyst recycling flow temperature from 127.5 °C to 120 °C, the flow rate of the diluted acid from the purification section from 561.3 kmol/h to 513.14 kmol/h and keeping the ratio of CO to methanol unchanged lead to a decrease in the WGSR rate and, as a result, the CO_2 production gets decreased by 34 %. In this research, it was explained that the temperature of the reactor cannot be lower than 180 °C, so investigating this issue and proposing a solution to it can be part of future research. Also, by examining and designing the reactor carefully, other parameters can be optimized to reduce the CO_2 production.

Nomenclature

E	activation energy [$\frac{kJ}{kmol}$].
F_{12}	feed ratio of CO to methanol.
[I]	Concentration of methyl Iodide [$\frac{kmol}{m^3}$].
i	numerators of the independent variables.
j	numerators of the independent variables.
K_0	reaction rate constant [$\frac{m^3}{kmol.s}$].
k	numerators of the independent variables.
L_C	liquid level.
m	degree of reaction to gas component.
n	degree of reaction to liquid component.
Q_R	flow rate of dilute acid stream [$\frac{kmol}{h}$].
Rate	reaction rate [$\frac{kmol}{m^3.s}$].
[Rh]	concentration of rhodium catalyst [$\frac{kmol}{m^3}$].
R	universal gas constant [$\frac{kJ}{K.kmol}$].
T	temperature [K].
T_R	temperature of the catalyst-rich recycle stream [K].
x	independent variable.
y	dependent variable.

Greek letters

β	matrix of coefficients.
ε	error value.

References

[1] Romanainen, J. J. and Salmi, T., "Numerical strategies in solving gas-liquid reactor models—1. Stagnant films and a steady state CSTR", *Computers & Chemical Engineering*, **15** (11), 769 (1991).

[2] Wang, J., Han, S., Wei, F., Yu, Z. and Jin, Y., "An axial dispersion model for gas–liquid reactors based on the penetration theory", *Chemical Engineering and Processing: Process Intensification*, **36** (4), 291 (1997).

[3] Markoš, J., Pisu, M. and Morbidelli, M., "Modeling of gas-liquid reactors: Isothermal semibatch and continuous stirred tank reactors", *Computers & Chemical Engineering*, **22** (4-5), 627 (1998).

[4] Trambouze, P. and Euzen, J. P., Chemical reactors: From design to operation, Editions Technip, Paris, (2004).

[5] Bao, Y., Yang, J., Wang, B. and Gao, Z., "Influence of impeller diameter on local gas dispersion properties in a sparged multi-impeller stirred tank", *Chinese Journal of Chemical Engineering*, **23** (4), 615 (2015).

[6] Da Silva, T. L., Calado, V., Silva, N., Mendes, R. L., Alves, S. S., Vasconcelos, J. M. and Reis, A., "Effects of hydrocarbon additions on gas-liquid mass transfer coefficients in biphasic bioreactors", *Biotechnology and Bioprocess Engineering*, **11** (3), 245 (2006).

[7] Behzadi, S. and Farid, M. M., "Production of biodiesel using a continuous gas–liquid reactor", *Bioresource Technology*, **100**

(2), 683 (2009).

[8] Ding, J., Wang, X., Zhou, X. F., Ren, N. Q. and Guo, W. Q., "CFD optimization of continuous stirred-tank (CSTR) reactor for biohydrogen production", *Bioresource Technology*, **101** (18), 7005 (2010).

[9] Liu, K., Phillips, J. R., Sun, X., Mohammad, S., Huhnke, R. L. and Atiyeh, H. K., "Investigation and modeling of gas-liquid mass transfer in a sparged and non-sparged continuous stirred tank reactor with potential application in syngas fermentation", *Fermentation*, **5** (3), 75 (2019).

[10] Johnson, M. D., May, S. A., Kopach, M. E., Groh, J. M. C., White, T. D., Cole, K. P. and Shankarraman, V., "Continuous reactors for pharmaceutical manufacturing", Continuous pharmaceutical processing, AAPS Advances in the pharmaceutical sciences series, Nagy, Z., El Hagrasy, A. and Litster, J. (eds.), Vol. 42, Springer, Cham, p. 23 (2020).

[11] Stoll, I. K., Boukis, N. and Sauer, J., "Syngas fermentation to alcohols: Reactor technology and application perspective", *Chemie Ingenieur Technik*, **92** (1-2), 125 (2020).

[12] Jensen, M. B., Ottosen, L. D. M. and Kofoed, M. V. W., "H_2 gas-liquid mass transfer: A key element in biological power-to-gas methanation", *Renewable and Sustainable Energy Reviews*, **147**, 111209 (2021).

[13] Nam, J. S., Kim, A. R., Kim, D. M., Chang, T. S., Kim, B. S. and Bae, J. W., "Novel heterogeneous Rh-incorporated graphitic-carbon nitride for liquid-phase carbonylation of methanol to AcOH", *Catalysis Communications*, **99**, 141 (2017).

[14] Kalck, P., Le Berre, C. and Serp, P., "Recent advances in the methanol carbonylation reaction into AcOH", *Coordination Chemistry Reviews*, **402**, 213078 (2020).

[15] Jiang, H., Liu, Z., Pan, P. and Yuan, G., "A novel supported catalyst for the carbonylation of methanol", *Journal of Molecular Catalysis A: Chemical*, **148** (1-2), 215 (1999).

[16] Schreck, D. J., Busby, D. C. and Wegman, R. W., "A highly efficient catalyst system for the isomerization of methyl formate to AcOH", *Journal of Molecular Catalysis*, **47** (1), 117 (1988).

[17] Huang, W., Xie, K. C., Wang, J. P., Gao, Z. H., Yin, L. H. and Zhu, Q. M., "Possibility of direct conversion of CH_4 and CO_2 to high-value products", *Journal of Catalysis*, **201** (1), 100 (2001).

[18] Ren, Z., Lyu, Y., Song, X. and Ding, Y., "Review of heterogeneous methanol carbonylation to acetyl species", *Applied Catalysis A: General*, **595**, 117488 (2020).

[19] Yoneda, N., Kusano, S., Yasui, M., Pujado, P. and Wilcher, S., "Recent advances in processes and catalysts for the production of AcOH", *Applied Catalysis A: General*, **221** (1-2), 253 (2001).

[20] Murphy, M. A., Smith, B. L., Torrence, G. P. and Aguilo, A., "Iodide and acetate promotion of carbonylation of methanol to AcOH: Model and catalytic studies", *Journal of Organometallic Chemistry*, **303** (2), 257 (1986).

[21] Smith, B. L., Torrence, G. P., Murphy, M. A. and Aguilo, A., "The rhodium-catalyzed methanol carbonylation to AcOH at low water concentrations: The effect of iodide and acetate on catalyst activity and stability", *Journal of*

Molecular Catalysis, **39** (1), 115 (1987).

[22] Haynes, A., Maitlis, P. M., Morris, G. E., Sunley, G. J., Adams, H., Badger, P. W. and Watt, R. J., "Promotion of iridium-catalyzed methanol carbonylation: Mechanistic studies of the cativa process", *Journal of the American Chemical Society*, **126** (9), 2847 (2004).

[23] Zhang, Q., He, A., Xiao, W., Du, J., Liu, Z. and Tao, C., "Non-aqueous liquid phase synthesis of AcOH via ionic liquid promoted homogeneous carbonylation of methanol over Ir (III) catalysts", *Bulletin of the Chemical Society of Japan*, **95** (3), 451 (2022).

[24] Ji, W., Zhang, S., Dong, F., Feng, N., Lan, L., Li, Y. and Sun, Y., "Study on Rh (I)-o-aminophenol catalyst catalyzed carbonylation of methanol to AcOH", *Arabian Journal for Science and Engineering*, 1 (2022).

[25] Dimian, A. C. and Kiss, A. A., "Novel energy efficient process for AcOH production by methanol carbonylation", *Chemical Engineering Research and Design*, **159**, 1 (2020).

[26] Caxiano, I. N., Junqueira, P. G., Mangili, P. V. and Prata, D. M., "Eco-efficiency analysis and intensification of the AcOH purification process", *Chemical Engineering and Processing-Process Intensification*, **147**, 107784 (2020).

[27] Dickinson, R. E. and Cicerone, R. J., "Future global warming from atmospheric trace gases", *Nature*, **319** (6049), 109 (1986).

[28] Afzal, S., Sengupta, D., Sarkar, A., El-Halwagi, M. and Elbashir, N., "Optimization approach to the reduction of CO_2 emissions for syngas production involving dry reforming", *ACS Sustainable Chemistry & Engineering*, **6** (6), 7532 (2018).

[29] Rostami, Z., Heidari, N., Rahimi, M. and Azimi, N., "Enhancing the thermal performance of a photovoltaic panel using nano-graphite/paraffin composite as phase change material", *Journal of Thermal Analysis and Calorimetry*, **147** (5), 3947 (2022).

[30] Medrano-García, J. D., Ruiz-Femenia, R. and Caballero, J. A., "Revisiting classic AcOH synthesis: Optimal hydrogen consumption and carbon dioxide utilization", *Computer Aided Chemical Engineering*, **46**, 145 (2019).

[31] Abdulgader, M., Yu, Q. J., Zinatizadeh, A. A., Williams, P. and Rahimi, Z., "Application of response surface methodology (RSM) for process analysis and optimization of milk processing wastewater treatment using multistage flexible fiber biofilm reactor", *Journal of Environmental Chemical Engineering*, **8** (3), 103797 (2020).

[32] Nam, H., Kim, J. H., Kim, H., Kim, M. J., Jeon, S. G., Jin, G. T. and Ryu, H. J., "CO_2 methanation in a bench-scale bubbling fluidized bed reactor using Ni-based catalyst and its exothermic heat transfer analysis", *Energy*, **214**, 118895 (2021).

[33] Guo, Y., Dong, S. and Zhou, D., "Optimization of the photocatalyst coating and operating conditions in an intimately coupled photocatalysis and biodegradation reactor: Towards stable and efficient performance", *Environmental Research*, **204**, 111971 (2022).

[34] Zainullin, R. Z., Zagoruiko, A. N., Koledina, K. F., Gubaidullin, I. M. and Faskhutdinova, R. I., "Multi-criterion optimization of a catalytic reforming reactor unit using a genetic algorithm",

Catalysis in Industry, **12** (2), 133 (2020).

[35] Agrawal, G., Chaudhary, A. and Pani, A. K., "Temperature optimization in non-isothermal tubular reactor using genetic algorithm", Proceedings of *3rd International Conference on Communication System, Computing and IT Applications (CSCITA)*, pp. 23-26 (2020).

[36] Zhang, L., Chen, L., Xia, S., Ge, Y., Wang, C. and Feng, H., "Multi-objective optimization for helium-heated reverse water gas shift reactor by using NSGA-II", *International Journal of Heat and Mass Transfer*, **148**, 119025 (2020).

[37] Pajak, M., Buchaniec, S., Kimijima, S., Szmyd, J. S. and Brus, G. A, "Multiobjective optimization of a catalyst distribution in a methane/steam reforming reactor using a genetic algorithm", *International Journal of Hydrogen Energy*, **46** (38), 20183 (2021).

[38] Pan, R., Martins, M. F. and Debenest, G., "Pyrolysis of waste polyethylene in a semi-batch reactor to produce liquid fuel: Optimization of operating conditions", *Energy Conversion and Management*, **237**, 114114 (2021).

[39] Mahmoudian, F., Moghaddam, A. H. and Davachi, S. M., "Genetic-based multi-objective optimization of alkylation process by a hybrid model of statistical and artificial intelligence approaches", *The Canadian Journal of Chemical Engineering*, **100** (1), 90 (2022).

[40] Chaudhari, P., Thakur, A. K., Kumar, R., Banerjee, N. and Kumar, A., "Comparison of NSGA-III with NSGA-II for multi objective optimization of adiabatic styrene reactor", *Materials Today: Proceedings*, **57**, 1509 (2022).

[41] Thakur, A. K., Gupta, S. K., Kumar, R., Banerjee, N. and Chaudhari, P., "Multi-objective optimization of an industrial slurry phase ethylene polymerization reactor", *International Journal of Chemical Reactor Engineering*, **20** (6), 649 (2022).

[42] Osat, M., Shojaati, F. and Hafizi, A. A, "Multi-objective optimization of three conflicting criteria in a methane tri-reforming reactor", *International Journal of Hydrogen Energy*, **48** (16), 6275 (2023).

[43] Golhosseini, R., Naderifar, A., Mohammadrezaei, A. and Nasr, M. J., "Reaction engineering studies of homogeneous rhodium-catalyzed methanol carbonylation in a laboratory semi-batch reactor", *International Journal of Chemical Reactor Engineering*, **10** (1), (2012).

[44] Haroun, Y., Legendre, D. and Raynal, L., "Direct numerical simulation of reactive absorption in gas–liquid flow on structured packing using interface capturing method", *Chemical Engineering Science*, **65** (1), 351 (2010).

[45] Jafari, O., Rahimi, M., Hosseini Kakavandi, F. and Azimi, N., "Cu (II) removal intensification using Fe_3O_4 nanoparticles under inert gas and magnetic field in a microchannel", *International Journal of Environmental Science and Technology*, **14** (8), 1651 (2017).

[46] Azimi, N., Rahimi, M. and Zangenehmehr, P., "Numerical study of mixing and mass transfer in a micromixer by stimulation of magnetic nanoparticles in a magnetic field", *Chemical Engineering & Technology*, **44** (6), 1084 (2021).

[47] Levenspiel, O., Chemical reaction

engineering, 3rd ed., John Wiley and Sons, New York, USA, p. 534 (1999).

[48] Waschler, R., "Nonlinear analysis of chemical processes with material and energy recycles", Doctoral dissertation, Shaker Aachen, (2005).

[49] Lindenbergh, J., Smits, E., Stegeman, M. and Van der Waal, S., "Production of acetic acid AcOH from methanol", *Chemical Process Design*, 3164 (1996).

[50] Thomas, C. M. and Süss-Fink, G., "Ligand effects in the rhodium-catalyzed carbonylation of methanol", *Coordination Chemistry Reviews*, **243** (1-2), 125 (2003).

[51] Whyman, R., Piet, W. N. M. and Van Leeuwen, "Homogeneous catalysis—understanding the art", *Kluwer, Dordrecht*, 2004, (UK), p. 407 (2005).

[52] Dake, S. B., Jaganathan, R. and Chaudhari, R. V., "New trends in the rate behavior of rhodium-catalyzed carbonylation of methanol", *Industrial & Engineering Chemistry Research*, **28** (7), 1107 (1989).

[53] Nowicki, L., Ledakowicz, S. and Zarzycki, R., "Kinetics of rhodium-catalyzed methanol carbonylation", *Industrial & Engineering Chemistry Research*, **31** (11), 2472 (1992).

[54] Beheshti, M. and Faizi, V., "Application of exergy analysis and response surface methodology (RSM) for reduction of exergy loss in AcOH production process", *Gas Processing Journal*, **3** (1), 51 (2015).

[55] Stempien, J. P., Ni, M., Sun, Q. and Chan, S. H., "Production of sustainable methane from renewable energy and captured carbon dioxide with the use of solid oxide electrolyzer: A thermodynamic assessment", *Energy*, **82**, 714 (2015).

[56] Davoodbeygi, Y. and Irankhah, A., "Nanostructured CeCu mixed oxide synthesized by solid state reaction for medium temperature shift reaction: Optimization using response surface method", *International Journal of Hydrogen Energy*, **43** (49), 22281 (2018).

[57] Golhosseini, R., Naderifar, A., Mohammadrezaei, A. R. and Jafari Nasr, M. R., "Kinetic study, modeling and simulation of homogeneous rhodium-catalyzed methanol carbonylation to AcOH", *Iranian Journal of Chemistry and Chemical Engineering*, **31** (1) 57 (2012).

[58] Jafari, A. A., Tourani, S. and Khorasheh, F., "Simulation of methanol carbonylation reactor in AcOH production plant: Selection of an appropriate correlation for mass transfer coefficients", *International Journal of Chemical Reactor Engineering*, **17** (4) 20180122 (2019).

[59] Bezerra, M. A., Santelli, R. E., Oliveira, E. P., Villar, L. S. and Escaleira, L. A., "Response surface methodology (RSM) as a tool for optimization in analytical chemistry", *Talanta*, **76** (5), 965 (2008).

[60] Valitabar, M., Rahimi, M. and Azimi, N., "Experimental investigation on forced convection heat transfer of ferrofluid between two-parallel plates", *Heat and Mass Transfer*, **56** (1), 53 (2020).

[61] Breig, S. J. M. and Luti, K. J. K., "Response surface methodology: A review on its applications and challenges in microbial cultures", *Materials Today: Proceedings*, **42**, 2277 (2021).

[62] Waschler, R., Kienle, A., Anoprienko, A. and Osipova, T., "Dynamic plantwide modelling, flowsheet simulation and nonlinear analysis of an industrial production plant", *Computer Aided Chemical Engineering*, **10**, 583 (2002).

[63] Baker, E. C., Hendriksen, D. E. and Eisenberg, R., "Mechanistic studies of the homogeneous catalysis of the water gas shift reaction by rhodium carbonyl iodide", *Journal of the American Chemical Society*, **102** (3), 1020 (1980).

[64] Bhatti, M. S., Kapoor, D., Kalia, R. K., Reddy, A. S. and Thukral, A. K., "RSM and ANN modeling for electrocoagulation of copper from simulated wastewater: Multi objective optimization using genetic algorithm approach", *Desalination*, **274** (1-3), 74 (2011).

[65] Hosseinpour, V., Kazemeini, M. and Mohammadrezaee, A., "A study of the water–gas shift reaction in Ru-promoted Ir-catalysed methanol carbonylation utilizing experimental design methodology", *Chemical Engineering Science*, **66** (20), 4798 (2011).